

## The (AgGa)<sub>1-z</sub>Mn<sub>2z</sub>Te<sub>2</sub> Alloys: Phase Relations and the Effects of Ordering

M. QUINTERO AND R. TOVAR

*Centro de Estudios de Semiconductores, Departamento de Física,  
Universidad de los Andes, Mérida, Venezuela*

AND M. AL-NAJJAR, G. LAMARCHE, AND J. C. WOOLLEY

*Ottawa-Carleton Institute of Physics, University of Ottawa,  
Ottawa, Ontario, K1N 6N5 Canada*

Received November 9, 1987

Polycrystalline samples of (AgGa)<sub>1-z</sub>Mn<sub>2z</sub>Te<sub>2</sub> alloys were prepared by the melt and anneal technique and were used in lattice parameter, optical energy gap  $E_0$ , and differential thermal analysis measurements. Both chalcopyrite  $\alpha$  and zinc blende  $\beta$  single-phase fields are found and the results indicate that in both of these cases ordering of the manganese can occur at lower temperatures to give ordered  $\alpha'$  and  $\beta'$  structures. The composition and temperature ranges of these fields are shown on a  $T(z)$  diagram. It is found that the manganese ordering has an appreciable effect on  $E_0$ . This is demonstrated by the different aiming points at  $z = 1.0$  for the  $E_0$  vs  $z$  lines in the different fields, the values being  $\sim 2.2$  eV for  $\alpha$ ,  $\sim 1.9$  eV for  $\beta'$ , and 1.35 eV for  $\alpha'$ . © 1988 Academic Press, Inc.

### Introduction

Semiconductor alloys containing paramagnetic manganese ions are of interest because of their magnetic as well as semiconductor properties. Pseudobinary alloys of the form II<sub>1-z</sub>Mn<sub>z</sub>VI, such as Cd<sub>1-z</sub>Mn<sub>z</sub>Te, have been investigated in much detail (1-4) and the work has been extended to pseudoternary alloys such as Cd<sub>x</sub>Zn<sub>y</sub>Mn<sub>z</sub>Te ( $x + y + z = 1$ ) (e.g., (5, 6)). In all of these alloys, the manganese ions are arranged at random on the cation sublattice and as a result the alloys show spin-glass behavior at low temperatures. These alloys have been given the names semimagnetic semiconductors or diluted magnetic semiconductors. Other possible semimagnetic al-

loys can be derived from the chalcopyrite I III VI<sub>2</sub> compounds, the ternary analogs of the II VI compounds. To retain the electron to atom ratio and thus the semiconductor properties, it is necessary to replace one I and one III cation simultaneously by two manganese atoms, so that the alloys of interest have the form (I III)<sub>1-z</sub>Mn<sub>2z</sub>Te<sub>2</sub> or in the more general pseudoternary case II<sub>2x</sub>(I III)<sub>y</sub>Mn<sub>2z</sub>Te<sub>2</sub> ( $x + y + z = 1$ ).

Lattice parameter and optical energy gap data have been obtained for the systems Cd<sub>2x</sub>(CuIn)<sub>y</sub>Mn<sub>2z</sub>Te<sub>2</sub> (7) and Cd<sub>2x</sub>(AgIn)<sub>y</sub>Mn<sub>2z</sub>Te<sub>2</sub> (8) and magnetic measurements made on various (I III)<sub>1-z</sub>Mn<sub>2z</sub>Te<sub>2</sub> alloys (9). The results indicate that ordering of the manganese ions on the cation sublattice occurs in these alloys and that this has a sig-

nificant effect on the magnetic behavior and on the optical energy gap values. In order to examine these effects in more detail, it is necessary to have information concerning the phase diagram and the ordered structure of those alloys. Aresti *et al.* (10) have used differential thermal analysis (DTA) measurements to give a  $T(z)$  phase diagram of the (CuIn)<sub>1-z</sub>Mn<sub>2z</sub>Te<sub>2</sub> system, but did not obtain any indication of ordering temperatures, etc. They suggest that in the range of chalcopyrite behavior, the manganese tends to order on a stannite type of arrangement.

In recent work (11), the  $T(z)$  diagram of (CuIn)<sub>1-z</sub>Mn<sub>2z</sub>Te<sub>2</sub> has been repeated to determine ordering temperature values in both the chalcopyrite and zinc blende fields and the corresponding  $T(z)$  diagram determined for the (AgIn)<sub>1-z</sub>Mn<sub>2z</sub>Te<sub>2</sub> case. It has been shown that while the lattice parameter values are not noticeably affected by the ordering of the manganese, the optical energy gap ( $E_0$ ) values in the ordered and disordered alloys are appreciably different and that the value of  $E_0$  is a good indication of the state of the alloy.

In the present work, the  $T(z)$  diagram, lattice parameter, and optical energy gap values of the (AgGa)<sub>1-z</sub>Mn<sub>2z</sub>Te<sub>2</sub> alloys have been investigated.

### Experimental Methods

Polycrystalline samples of the alloys were prepared from the elements by the melt and anneal technique (7). The annealing temperature to be used was uncertain until the  $T(z)$  diagram had been determined, but annealing at 600°C for about 20 days followed by slow cooling to room temperature gave good single-phase samples for the initial work. (With the furnace switched off at 600°C, cooling to room temperature took about 10 hr). Other heat treatment conditions to vary the value of  $E_0$  will be mentioned below. Debye-Scherrer powder X-

ray photographs were taken to determine the phase condition and lattice parameter values for the various samples.

DTA measurements (12) were made for a range of sample compositions, with 50–100 mg specimens being used. Since the work was part of a program for the investigation of semimagnetic semiconductor alloys, the range of composition investigated was limited to  $0 \leq z \leq 0.7$  and the behavior of the MnTe-rich phases was not considered. Thus a maximum temperature of 1000°C was sufficient for the work and silver was used as the reference material. Heating and then cooling runs were carried out on each sample investigated.

Room temperature optical energy gap ( $E_0$ ) values were measured by the usual optical absorption method (13). For each sample, a slice was polished down to a thickness  $d$  in the range 50–150  $\mu\text{m}$ . The variations of  $I_0$ , the intensity of the incident radiation, and  $I_t$ , the transmitted intensity, were determined as a function of photon energy  $h\nu$  and values of  $1/d \ln I_0/I_t$  found. These values were corrected by subtracting a background value to give the absorption coefficient  $\alpha$  and the relation  $\alpha h\nu = A(E_0 - h\nu)^{1/2}$  was then used to give a value for  $E_0$ .

### Phase and Crystallographic Results

The results of the DTA measurements are shown by the points in Fig. 1, where heating and cooling data are indicated separately. The proposed phase boundaries determined from these points are shown as full lines. The dashed lines show phase boundaries estimated with the help of X-ray and optical energy gap results. In Fig. 1, the values at  $z = 0$ , i.e., AgGaTe<sub>2</sub>, are in good agreement with the results of Palatnik and Belova (14), for the AgGaTe<sub>2</sub> point in the Ag<sub>2</sub>Te–Ga<sub>2</sub>Te<sub>3</sub> diagram. In the present work,  $\alpha$  is the chalcopyrite phase,  $\beta$  the zinc blende phase, and  $\gamma$  the hexagonal NiAs structure of MnTe. As is seen from

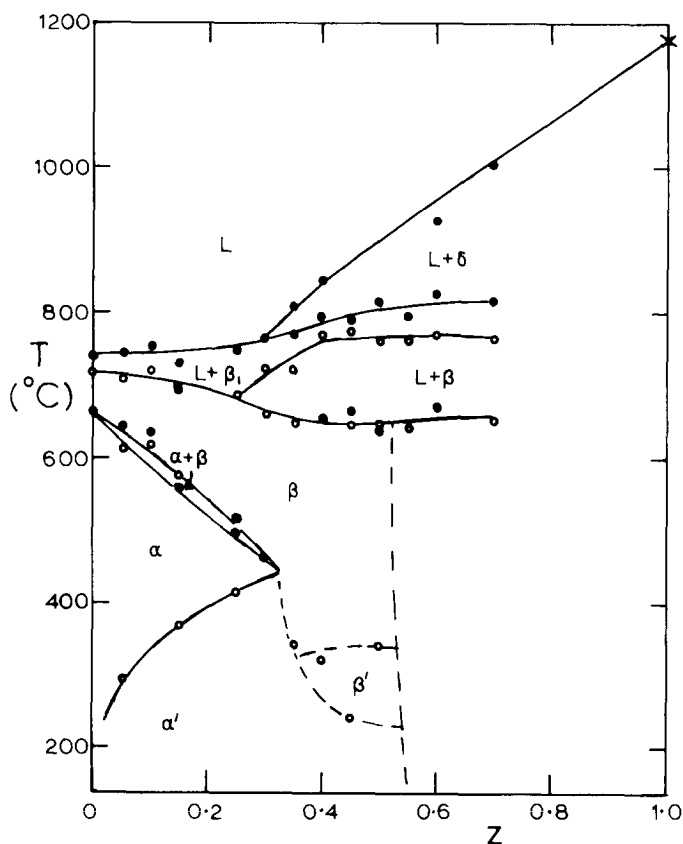


FIG. 1.  $T(z)$  diagram for  $(\text{AgGa})_{1-z}\text{Mn}_{2z}\text{Te}_2$  alloys.  $\circ$ , Heating run;  $\bullet$ , cooling run.

the diagram of Palatnik and Belova, two different zinc blende fields are present, accounting for the  $\beta$  and  $\beta_1$  phases in the present diagram. By comparison with the  $(\text{CuIn})_{1-z}\text{Mn}_{2z}\text{Te}_2$  diagram (10), the  $\delta$  phase has the rock salt structure shown by MnTe above  $1050^\circ\text{C}$  but which exists at lower temperatures elsewhere in the general diagram. The present section is clearly not pseudobinary.

The ordering of manganese on the cation sublattice occurs in both the chalcopyrite and zinc blende structures, the ordered fields being labeled  $\alpha'$  and  $\beta'$ , respectively. Estimates based on ordering line positions in the  $(\text{AgIn})_{1-z}\text{Mn}_{2z}\text{Te}_2$  alloys (11) indicate that the manganese atoms probably lie on

planes perpendicular to the  $c$  axis. The ordered structure of that system plus the present one is being investigated in more detail by neutron diffraction work.

For sample slowly cooled to room temperature after annealing, the X-ray photographs showed the samples to be either single-phase chalcopyrite or two-phase chalcopyrite plus the hexagonal MnTe structure, i.e., as shown in Fig. 1 there is no zinc blende field at the lower temperatures. Lattice parameter values were determined for the chalcopyrite phase in the different samples and it was found that the variation of  $a$  with  $z$  was of the same magnitude as the experimental scatter in the values. This small variation is not unexpected in this

case, since the results for (CuIn)<sub>1-z</sub>Mn<sub>2z</sub>Te<sub>2</sub> (7) and (AgIn)<sub>1-z</sub>Mn<sub>2z</sub>Te<sub>2</sub> (8) indicate that the value of  $a$  extrapolated to  $z = 1.0$  is 0.6333 nm. The value of  $a$  obtained here for AgGaTe<sub>2</sub> is 0.6326 nm, so that little variation of  $a$  with  $z$  is to be expected. Thus the usual method of using a discontinuity in slope of the  $a$  vs  $z$  curve to find the limit of the single-phase field cannot be used in this case. However, the optical energy gap data given below indicates that the  $z = 0.5$  alloy is single phase while the X-ray photograph of the  $z = 0.6$  alloy clearly shows lines of the MnTe phase. Thus in Fig. 1, the phase boundary at lower temperature has been taken at  $z = 0.55$ .

The value of  $c/a$  also remained constant over the range of chalcopyrite structure with values in the range 1.900–1.905. This is in contrast to the results for the (AgIn)<sub>1-z</sub>Mn<sub>2z</sub>Te<sub>2</sub> alloys (8), where  $c/a$  increased toward 2 as  $z$  increased and the alloys showed zinc blende structure in the range  $0.38 \leq z \leq 0.72$ .

### Optical Energy Gap Results

The room temperature values of  $E_0$  as a function of  $z$  and for various heat treatments are shown in Fig. 2. First, for samples cooled slowly from the annealing temperature to room temperature, and thus having the Mn-ordered chalcopyrite structure  $\alpha'$ , it is seen that  $E_0$  shows a linear variation with  $z$  and extrapolates at  $z = 1$  to a value of  $E_0 = 1.35$  eV. This is in good agreement with the results for the (CuIn)<sub>1-z</sub>Mn<sub>2z</sub>Te<sub>2</sub> and (AgIn)<sub>1-z</sub>Mn<sub>2z</sub>Te<sub>2</sub> alloys which both showed this same aiming point for  $E_0$  values in the Mn-ordered chalcopyrite  $\alpha'$  range. In the composition range  $0 \leq z \leq 0.2$ , it was found that samples air-quenched from 500°C gave a different set of  $E_0$  values, which show an aiming point at  $z = 1$  of  $E_0 \sim 2.2$  eV. This is obviously the value for the Mn-disordered chalcopyrite  $\alpha$  alloy. It has been shown previously (5, 7,

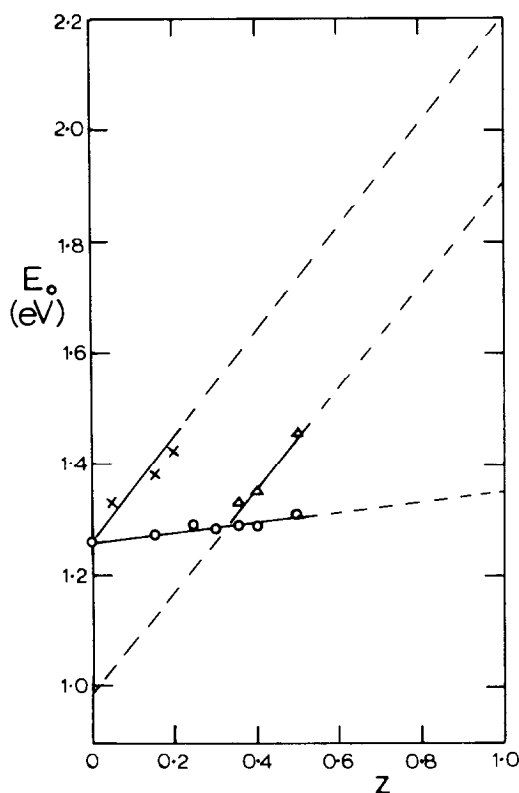


FIG. 2. Variation of room temperature optical energy gap  $E_0$  with  $z$  for (AgGa)<sub>1-z</sub>Mn<sub>2z</sub>Te<sub>2</sub> alloys. ○, Samples slowly cooled to room temperature; ×, samples air quenched from 500°C; △, samples water quenched from 600°C.

11) that for the Mn-disordered zinc blende materials, the aiming point at  $z = 1$  is  $E_0 = 2.8$  eV and so an attempt was made in the present case to produce Mn-disordered zinc blende  $\beta$  alloys by quenching from 600°C. It was found however that rapid quenching in water did not retain the Mn-disordered form and for samples in the range  $0.3 \leq z \leq 0.5$ , values of  $E_0$  were obtained, as seen in Fig. 2, which showed an aiming point of  $E_0 \sim 1.95$  eV. As found previously (7, 8), this is the aiming point of the Mn-ordered zinc blende phase  $\beta'$ . Thus the  $z = 0.35$  alloy can take the  $\beta'$  form. The  $\beta$  and  $\beta'$  boundaries in Fig. 1 were drawn with this fact in mind.

If these zinc blende  $\beta'$  values are extrapolated to  $z = 0$ , a value of  $E_0 \sim 1.0$  eV is obtained, as the energy gap which  $\text{AgGeTe}_2$  would have in the zinc blende form. Similar extrapolations for the  $\text{AgInTe}_2$  and  $\text{CuInTe}_2$  cases gave values of  $\sim 0.7$  eV. Thus in all three cases, the difference between measured gap of the chalcopyrite compound and that extrapolated for the zinc blende form is  $\sim 0.25$  eV.

### Conclusions

The results obtained for the  $(\text{AgGa})_{1-z}\text{Mn}_{2z}\text{Te}_2$  alloys show that a wide range of solid solution occurs for both the chalcopyrite and zinc blende structures and that for both structures an ordered form, attributed to the manganese ions ordering on the cation sublattice, occurs in the range 300–400°C. In contrast to the  $(\text{CuIn})_{1-z}\text{Mn}_{2z}\text{Te}_2$  and  $(\text{AgIn})_{1-z}\text{Mn}_{2z}\text{Te}_2$  cases (II), the zinc blende field does not extend down to the room temperature range and all alloys produced by slow cooling show the chalcopyrite form.

The Mn-ordering has an appreciable effect on the optical energy gap values and the value of  $E_0$  is a good indication of the state of the alloy. Extrapolation of the measured  $E_0$  values to  $z = 1$  gives a value characteristic of the particular structure as shown previously (II). These values are 1.35 eV for the Mn-ordered chalcopyrite  $\alpha'$ ,  $\sim 2.2$  eV for the Mn-disordered chalcopyrite  $\alpha$ ,  $\sim 1.9$  eV for the Mn-ordered zinc blende  $\beta'$ , and 2.8 eV for the Mn-disordered  $\beta$  structures. Extrapolation to  $z = 0$  indicates that  $E_0 \sim 1.0$  eV for the hypothetical  $\text{AgGaTe}_2$  in the zinc blende form, giving

good correlation with similar values obtained for  $\text{AgInTe}_2$  and  $\text{CuInTe}_2$  (II).

### Acknowledgment

Two of the authors (M.Q. and R.T.) thank Consejo de Desarrollo Científico Humanístico y Tecnológico (CDCHT) Venezuela for financial support.

### References

1. J. K. FURDYNA, *J. Appl. Phys.* **53**, 6737 (1982).
2. J. A. GAJ, *J. Phys. Soc. Japan* **49**, 797 (1980).
3. R. R. GALAZKA, *Inst. Phys. Conf. Ser.* **43**, 133 (1979).
4. J. MYCIELSKI, *Prog. Cryst. Growth Charact.* **10**, 101 (1985).
5. R. BRUN DEL RE, T. DONOFRIO, J. E. AVON, J. MAJID, AND J. C. WOOLLEY, *Il Nuovo Cimento D* **2**, 1911 (1983).
6. T. DONOFRIO, G. LAMARCHE, AND J. C. WOOLLEY, *J. Appl. Phys.* **57**, 1932 (1985).
7. M. QUINTERO, L. DIERKER, AND J. C. WOOLLEY, *J. Solid State Chem.* **63**, 110 (1986).
8. M. QUINTERO AND J. C. WOOLLEY, *Phys. Status Solidi A* **92**, 449 (1985).
9. J. C. WOOLLEY, G. LAMARCHE, A. MANOOGIAN, M. QUINTERO, L. DIERKER, M. AL-NAJJAR, D. PROULX, C. NEAL, AND R. GOUDREULT, *In "Proceedings, 7th International Conference on Ternary and Multinary Compounds,"* Materials Research Society, p. 479 (1987).
10. A. ARESTI, L. GABARTO, A. GEDDO-LEHMANN, AND P. MANCA, *In "Proceedings, 7th International Conference on Ternary and Multinary Compounds,"* Materials Research Society, p. 497 (1987).
11. M. QUINTERO, P. GRIMA, R. TOVAR, G. S. PEREZ, AND J. C. WOOLLEY, in press.
12. R. CHEN AND Y. KIRSH, "Analysis of Thermally Stimulated Processes" (*Int. Series on Sol. State*, Vol. 15), p. 97, Pergamon, Elmsford, NY (1981).
13. R. G. GOODCHILD, O. H. HUGHES, S. A. LOPEZ-RIVERA, AND J. C. WOOLLEY, *Canad. J. Phys.* **60**, 1096 (1982).
14. L. S. PALATNIK AND E. K. BELOVA, *Inorg. Mater.* **3**, 1914 (1967).